Kroon, D., Zachos, J.C., and Richter, C. (Eds.)
Proceedings of the Ocean Drilling Program, Scientific Results Volume 208

3. DATA REPORT: CALCAREOUS NANNOFOSSIL BIOSTRATIGRAPHY OF THE PALEOCENE/EOCENE BOUNDARY, OCEAN DRILLING PROGRAM LEG 208 HOLE 1266C[1]

Simonetta Monechi[2] and Eugenia Angori[2]

INTRODUCTION

Ocean Drilling Program Leg 208 Hole 1266C (28°32.55′S, 2°20.61′E) is located along the northwestern flank of Walvis Ridge (South Atlantic Ocean). The location of Site 1266, at 3.798 km water depth, corresponds to a mid-depth site of the Leg 208 transect (Fig. **F1**). A stratigraphically continuous and expanded sequence of upper Paleocene and lower Eocene pelagic nannofossil ooze was recovered. Three holes were cored at Site 1266, and from Hole 1266C, an expanded and continuous Paleocene/Eocene (P/E) transition was recovered using the advanced piston corer system. The successful recovery and well-preserved nannofossil assemblages make Hole 1266C a reference section for improving the knowledge of the Paleocene/Eocene Thermal Maximum. The P/E transition is one of the most remarkable and intensively investigated time intervals. Significant and dramatic changes in climate and oceanography occurred at this transition. The P/E boundary is linked with an important turnover in benthic foraminifers and planktonic marine communities (Thomas and Shackleton, 1996; Kelly et al., 1998; Monechi et al., 2000; Bralower, 2002). This report documents the calcareous nannofossil assemblage fluctuations at the P/E boundary in Hole 1266C based on semiquantitative and quantitative investigations.

F1. Site 1266, p. 5.

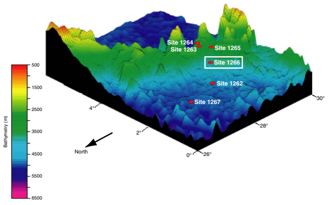

---

[1] Monechi, S., and Angori, E., 2006. Data report: calcareous nannofossil biostratigraphy of the Paleocene/Eocene boundary, Ocean Drilling Program Leg 208 Hole 1266C. *In* Kroon, D., Zachos, J.C., and Richter, C. (Eds.), *Proc. ODP, Sci. Results,* 208: College Station, TX (Ocean Drilling Program), 1–9. doi:10.2973/odp.proc.sr.208.203.2006

[2] Dipartimento di Scienze della Terra, Università degli Studi di Firenze, Via la Pira 4, I-50121 Firenze, Italy. Correspondence author: **monechi@unifi.it**

Initial receipt: 1 August 2005
Acceptance: 11 July 2006
Web publication: 6 December 2006
Ms 208SR-203

MATERIAL AND METHODS

The P/E boundary is marked by an abrupt contact between upper Paleocene nannofossil ooze and lower Eocene dusky red zeolite- and nannofossil-bearing clay that grades upward into nannofossil ooze (Zachos, Kroon, Blum, et al., 2004). The P/E boundary layer was recovered in Section 208-1266C-17H-3 at 306.8 meters composite depth (mcd). A 2.5-m-thick interval from Sections 208-1266C-17H-3 through 17H-2 was investigated for calcareous nannofossils. Semiquantitative investigations were carried out every centimeter across the P/E clay layer (from Sample 208-1266C-17H-3, 115–116 cm, to 17H-3, 84–85 cm), every 2 cm from Samples 17H-3, 149–150 cm, to 17H-3, 54–55 cm, and from this level upward from 3 to 20 cm.

Smear slides were prepared from unprocessed samples according to standard technical preparation methodology. Each smear slide was examined with a light microscope under 1250× magnification. Two traverses of each smear slide were checked for common and very rare species (Table **T1**). The relative abundance of each nannofossil taxon is defined as follows:

T1. Calcareous nannofossils, p. 7.

A = abundant (>30% of the total assemblages),
C = common (>10%–30% of the total assemblages),
F = few (>3%–10% of the total assemblages),
R = rare (1%–3% of the total assemblages), and
RR = very rare (<1% of the total assemblages).

The total abundance of nannofossils in each sample as estimated as follows:

V = very abundant (>30 specimens per field of view [FOV]),
A = abundant (>20–30 specimens per FOV),
C = common (>10–20 specimens per FOV),
F = few (>5–10 specimens per FOV),
R = rare (1–5 specimens per FOV),
RR = very rare (<1 specimen per FOV), and
B = barren of nannofossils.

Preservation of nannofossils was recorded using the criteria of Steinmetz (1979) as good (G), moderate (M), and poor (P). Depths of samples in the range chart are reported in meters composite depth (Zachos, Kroon, Blum, et al., 2004).

RESULTS

The biostratigraphic zonation used to divide the Paleocene–Eocene interval is based on the calcareous nannofossil events defined by Martini (1971). In order to define the base of Zone NP10, characterized by the first occurrence (FO) of *Rhomboaster bramlettei*, we followed the definition of Bybell and Self-Trail (1995), who included *Rhomboaster cuspis* of many authors with *R. bramlettei*. In addition, we adopted the taxonomic remarks of Angori and Monechi (1996), who differentiated three morphotypes of *R. bramlettei* (*R. bramlettei* “short arms,” *R. bramlettei* “long arms,” and *R. bramlettei* var. T). The studied interval spans from Zones NP9 to NP10. The upper Paleocene nannofossil assemblages are mainly composed of *Coccolithus pelagicus, Toweius pertusus, Fasciculithus* *tympaniformis, Sphenolithus,* and *Discoaster multiradiatus*. At the P/E boundary, the base of the clay interval, the total nannofloral abundance sharply decreases and an enhancement of dissolution occurs from Sample 208-1266C-17H-3, 112–113 cm, to 17H-3, 98–99 cm. Within this interval the FO of *R. bramlettei* s.a. was detected in Sample 208-1266C-17H-3, 107–108 cm, where the base of Zone NP10 was recognized. Long rays, asymmetrical, and prominent-stem discoaster species such as *Discoaster anartios*, *Discoaster araneus*, *Discoaster* cf. *Discoaster lodoensis, Discoaster salisburgensis*, and *Discoaster diastypus* also have FOs in this interval, as previously documented by Monechi et al. (2000), Kahn and Aubry (2004), and Angori et al. (submitted [**N1**]). The FO of *Fasciculithus thomasii* has been recorded at the carbon isotope excursion onset. The genus *Rhomboaster* is not very common, but several morphotypes of the *Rhomboaster-Tribrachiatus* lineage were recognized (Table **T1**). Furthermore, significant changes in the calcareous nannofossil assemblages were observed: (1) an increase in the relative abundance of dissolution-resistant forms such as *Discoaster multiradiatus*, *Sphenolithus primus,* and *Fasciculithus tympaniformis*; (2) a decrease in the relative abundance of *C. pelagicus* and *T. pertusus;* and (3) the absence of *Zygrhablithus bijugatus*. From Sample 208-1266C-17H-3, 101–102 cm, upward, an opposite trend between *D. multiradiatus* and *F. tympaniformis* was noted. *D. multiradiatus* decreases from abundant to few, whereas *F. tympaniformis* increases from common to abundant up to Sample 208-1266C-17H-3, 57–58 cm, where *Fasciculithus* decreases. Above this level, only *F. tympaniformis* is always present throughout the studied interval but in very low abundances. At approximately the same level (Sample 208-1266C-17H-3, 63–64 cm) as the decrease of *Fasciculithus,* the holococcolith species *Z. bijugatus* exhibits a significant abundance increase, as observed in several tethyan sections and at high latitudes (Monechi et al., 2000; Bralower, 2002; Orue-Etxebarria et al., 2004; Tremolada and Bralower 2004). The *Fasciculithus/Zyghrablithus* crossover (N3 event of Zachos et al., 2005) has been placed at 306.28 mcd. *Z. bijugatus* increases considerably, becoming one of the most abundant taxa together with *C. pelagicus, S. primus,* and *T. pertusus*. The genus *Toweius* above the P/E boundary does not reach the same abundances as in the preboundary interval. See Plate **P1** for examples of nannofossils found at Site 1266.

P1. Calcareous nannofossils, p. 6.

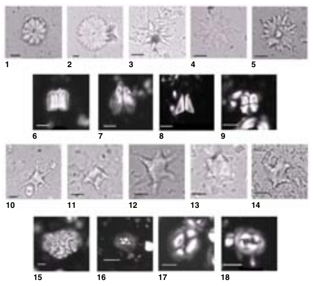

ACKNOWLEDGMENTS

This research used samples and data provided by the Ocean Drilling Program (ODP). ODP is sponsored by the U.S. National Science Foundation (NSF) and participating countries under management of Joint Oceanographic Institutions (JOI), Inc. This study was supported by Cofin 2003 to S. Monechi. We thank Viviana Reale for assistance in sample preparations.

REFERENCES

Angori, E., and Monechi, S., 1996. High-resolution calcareous nannofossil biostratigraphy across the Paleocene/Eocene boundary at Caravaca (southern Spain). *Israel J. Earth Sci.,* 44:197–206.

Bralower, T.J., 2002. Evidence for surface water oligotrophy during the late Paleocene–Eocene Thermal Maximum: nannofossil assemblages data from Ocean Drilling Program Site 690, Maud Rise, Weddell Sea. *Paleoceanography,* 17(2):1–12. **doi:10.1029/2001PA000662**

Bybell, L.M., and Self-Trail, J.M., 1995. Evolutionary, biostratigraphic, and taxonomic study of calcareous nannofossils from a continuous Paleocene/Eocene boundary section in New Jersey. *Geol. Surv. Prof. Pap. U.S.,* 1554.

Kahn, A., and Aubry, M.-P., 2004. Provincialism associated with the Paleocene/Eocene Thermal Maximum: temporal constraint. *Mar. Micropaleontol.,* 52(1–4):117–131. **doi:10.1016/j.marmicro.2004.04.003**

Kelly, D.C., Bralower, T.J., and Zachos, J.C., 1998. Evolutionary consequences of the latest Paleocene Thermal Maximum for tropical planktonic foraminifera. *Palaeogeogr., Palaeoclimatol., Palaeoecol.,* 141(1–2):139–161. **doi:10.1016/S0031-0182(98)00017-0**

Martini, E., 1971. Standard Tertiary and Quaternary calcareous nannoplankton zonation. *In* Farinacci, A. (Ed.), *Proc. 2nd Int. Conf. Planktonic Microfossils Roma:* Rome (Ed. Tecnosci.), 2:739–785.

Monechi, S., Angori, E., and von Salis, K., 2000. Calcareous nannofossil turnover around the Paleocene/Eocene transition at Alamedilla (southern Spain). *Bull. Soc. Geol. Fr.,* 171:477–489.

Orue-Etxebarria, X., Bernaola, G., Baceta, J.I., Angori, E., Caballero, F., Monechi, S., Pujalte, V., Dinarès-Turell, J., Apellaniz, E., and Payros, A., 2004. New constraints on the evolution of planktic foraminifera and calcareous nannofossils across the Paleocene–Eocene boundary interval: the Zumaia section revisited. *Neues Jahrb. Geol. Palaeontol., Abh.,* 234:223–259.

Steinmetz, J.C., 1979. Calcareous nannofossils from the North Atlantic Ocean, Leg 49, Deep Sea Drilling Project. *In* Luyendyk, B.P., Cann, J.R., et al., *Init. Repts. DSDP,* 49: Washington (U.S. Govt. Printing Office), 519–531.

Thomas, E., and Shackleton, N., 1996. The Palaeocene–Eocene benthic foraminiferal extinction and stable isotope anomalies. *In* Knox, R.W.O'B., Corfield, R.M., and Dunay, R.E. (Eds.), *Correlation of the Early Paleogene in Northwest Europe.* Geol. Soc. Spec. Publ., 101:401–441.

Tremolada, F., and Bralower, T.J., 2004. Nannofossil assemblage fluctuations during the Paleocene–Eocene Thermal Maximum at Sites 213 (Indian Ocean) and 401 (North Atlantic Ocean): paleoceanographic implications. *Mar. Micropaleontol.,* 52(1–4):107–116. **doi:10.1016/j.marmicro.2004.04.002**

Zachos, J.C., Kroon, D., Blum, P., et al., 2004. *Proc. ODP, Init. Repts.,* 208: College Station, TX (Ocean Drilling Program). **doi:10.2973/odp.proc.ir.208.2004**

Zachos, J.C., Röhl, U., Schellenberg, S.A., Sluijs, A., Hodell, D.A., Kelly, D.C., Thomas, E., Nicolo, M., Raffi, I., Lourens, L.J., McCarren, H., and Kroon, D., 2005. Rapid acidification of the ocean during the Paleocene–Eocene Thermal Maximum. *Science,* 308(5728):1611–1615. **doi:10.1126/science.1109004**

Figure F1. Three-dimensional diagram of Site 1266 location.

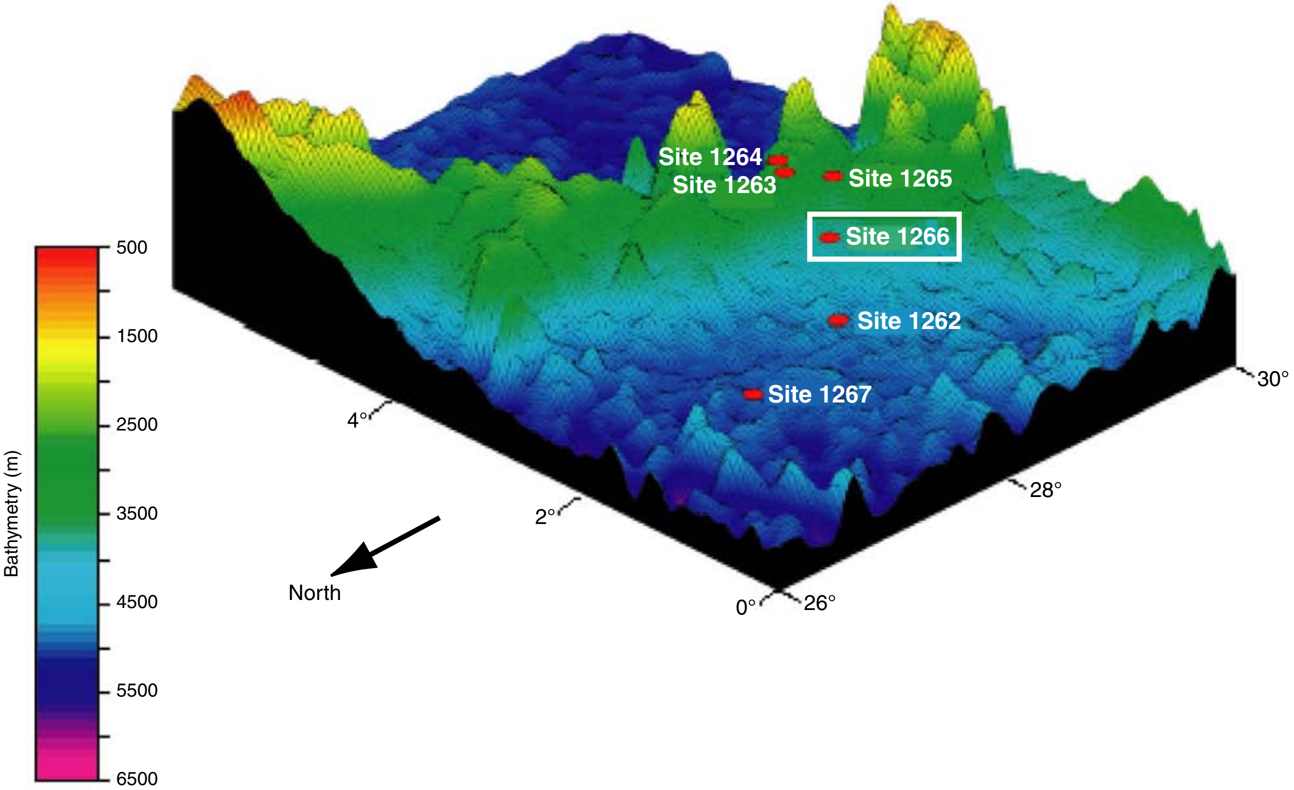

Plate P1. Calcareous nannofossils at Site 1266. XP = cross-polarized light, PL = plain transmitted light. Scale bar = 5 mm. (**1**) *Discoaster mohleri,* Sample 208-1266C-17H-3, 111–112 cm; PL. (**2**) *Discoaster multiradiatus,* Sample 208-1266C-17H-3, 111–112 cm; PL. (**3**) *Discoaster nobilis,* Sample 208-1266C-17H-3, 99–100 cm; PL. (**4**) *Discoaster araneus,* Sample 208-1266C-17H-3, 85–86 cm; PL. (**5**) *Discoaster anartios,* Sample 208-1266C-17H-3, 99–100 cm; PL. (**6**) *Fasciculithus tympaniformis*, Sample 208-1266C-17H-3, 95–96 cm; XP. (**7**) *Fasciculithus alanii,* Sample 208-1266C-17H-3, 98–99 cm; XP. (**8**) *Fasciculithus clinatus,* Sample 208-1266C-17H-3, 98–99 cm; XP. (**9**) *Sphenolithus primus,* Sample 208-1266C-17H-3, 96–97 cm; XP. (**10**) *Rhomboaster bramlettei* l.a., Sample 208-1266C-17H-3, 83–84 cm; PL. (**11**) *R. bramlettei* s.a., Sample 208-1266C-17H-3, 104–105 cm; PL. (**12**) *R. bramlettei* l.a., Sample 208-1266C-17H-3, 91–92 cm; PL. (**13**) *R. bramlettei* var. T, Sample 208-1266C-17H-3, 78–79 cm; PL. (**14**) *Rhomboaster* cf. *Rhomboaster contortus,* Sample 208-1266C-17H-3, 71–72 cm; PL. (**15**) *Thoracosphaera saxea,* Sample 208-1266C-17H-3, 89–90 cm; XP. (**16**) *Biscutum* sp., Sample 208-1266C-17H-3, 89–90 cm; XP. (**17**) *Coccolithus pelagicus,* Sample 208-1266C-17H-3, 96–97 cm; XP. (**18**) *Toweius pertusus,* Sample 208-1266C-17H-3, 83–84 cm; XP.

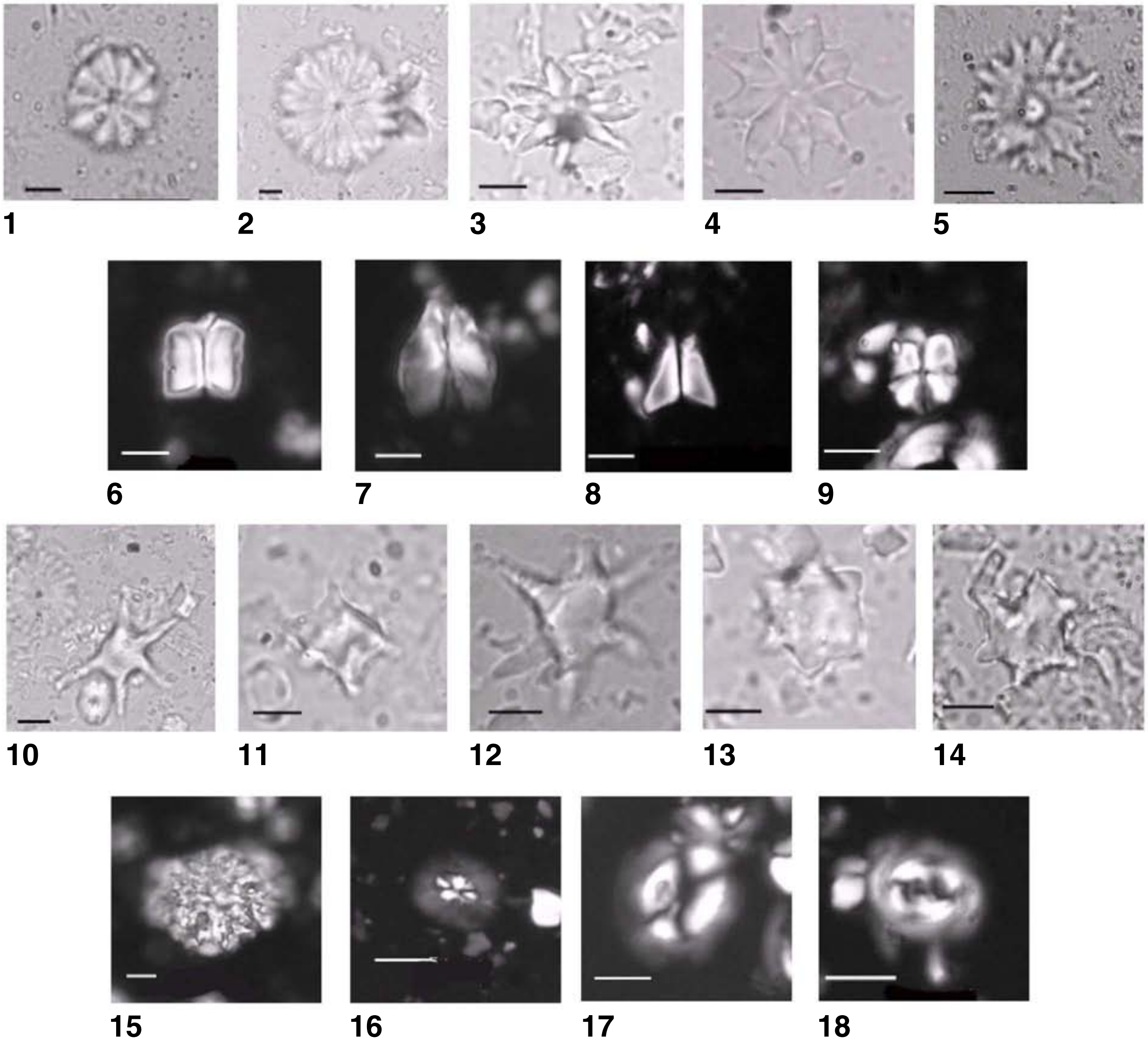

Table T1. Distribution of selected calcareous nannofossils at the Paleocene/Eocene boundary, Hole 1266C. (**See table notes.** Continued on next page.)

Core, section, interval (cm)	Depth (mcd)	Nannofossil zone	Total abundance	Preservation	*Biantholithus* spp.	*Biscutum* spp.	*Braarudosphaera* spp.	*Campylosphaera* spp.	*Chiasmolithus bidens*	*Chiasmolithus consuetus*	*Chiasmolithus solitus*	*Chiasmolithus* spp.	*Coccolithus pelagicus*	*Coccolithus* spp.	*Cruciplacolithus* spp.	*Discoaster anartios*	*Discoaster araneus*	*Discoaster lenticularis*	*Discoaster mohleri*	*Discoaster multiradiatus*	*Discoaster nobilis*	*Discoaster diastypus*	*Discoaster* cf. *D. lodoensis*	*Discoaster salisburgensis*	*Ellipsolithus distichus*	*Ellipsolithus macellus*	*Ericsonia* spp.	*Fasciculithus alanii*	*Fasciculithus clinatus*	*Fasciculithus hayi*	*Fasciculithus involutus*	*Fasciculithus thomasii*	*Fasciculithus tympaniformis*	*Fasciculithus* spp.	*Hornibrookina* spp.	*Markalius* spp.	*Neochiastozygus* spp.	*Neococcolithes* spp.	*Pontosphaera* spp.	*Prinsius* spp.	*Rhomboaster bramlettei* s.a.	*Rhomboaster bramlettei* l.a.	*Rhomboaster bramlettei* var. T	*Rhomboaster* cf. *R. contortus*	*Sphenolithus anarrhopus*	*Sphenolithus moriformis*	*Sphenolithus primus*	*Thoracosphaera* spp.	*Toweius eminens*	*Toweius pertusus*	*Toweius* spp.	*Tribrachiatus* cf. *T. digitalis*	*Placozygus* spp.	*Zygrhablithus bijugatus*
208-1266C-																																																						
17H-2, 46–47	304.61	NP 10	V	M	R	RR		R	F	RR	RR	F	A	F						F	F												R	R		RR				RR						F	F	RR		C			RR	A
17H-2, 58–59	304.73		V	M		RR			F	R	RR	R	A	R	R				R	F	R												R	R					RR							RR	R	RR		C			RR	A
17H-2, 70–71	304.85		V	M		cf					RR	R	A	R					R	C	R												F	F		RR										F	F			C	RR		RR	A
17H-2, 91–92	305.06		V	M		RR		R	RR	R	R	R	A	F	R				R	C	F				RR								F	F		R		RR	RR							F	F			C			RR	C
17H-2, 106–107	305.21		V	M		RR		R		R	RR	F	A	R	R					C	R				RR								F	F					R								R	RR	R	C			R	A
17H-2, 118–119	305.33		V	M		cf		F	F	RR	RR	F	A	R	R				RR	C	RR				RR								F	F		RR	RR			RR						F	F	RR	R	C			R	C
17H-2, 127–128	305.42		V	M		RR		R	RR	R	RR	F	A	F	R			RR	RR	C	R												F	F	RR	R			RR							F	F		R	C			RR	C
17H-2, 139–140	305.54		V	M		RR		RR	F	RR	RR	F	A	R	R				RR	C	F					RR							F	F		RR			RR				RR			RR	F			C				A
17H-3, 4–5	305.69		V	M		cf		R	RR	RR	R	R	A	R	R					F	F					RR							R	R	R	R		RR	RR				RR			RR	F	RR	R	F	F	RR	RR	C
17H-3, 19–20	305.84		V	M	R	RR		R	RR	R	RR	R	A	R	F				RR	C	C												R	R		RR			RR		RR					RR	F	RR	F	C	R	RR	RR	A
17H-3, 28–29	305.93		V	M		RR		F	RR	R	RR	R	A	RR	RR					F	F	RR											R	F		RR										RR	F		F	C			RR	A
17H-3, 33–34	305.98		V	M				R	F	R	R	R	A	F	R					F	F						RR						R	R									RR			F	F	RR	F	C		RR	R	A
17H-3, 37–38	306.02		C	M		RR		R	F	R	RR	R	A	R	R				RR	F	R												F	RR		R								RR			F	RR	F	C			RR	A
17H-3, 40–41	306.05		V	M	RR	RR		R		R	R	R	A	RR	R					C	F						RR						F	F		RR										F	F	RR	R	C				A
17H-3, 43–44	306.08		V	M	R	RR	RR	F		RR	RR	RR	A	R	F					F	F					R	RR						RR	RR		RR										RR	F		F	C			RR	A
17H-3, 46–47	306.11		V	M	RR			RR	F	R	RR	F	A	R	F					C	F						RR						R	R		RR				RR	RR				RR		F	RR	R	C				A
17H-3, 51–52	306.16		V	M	RR	RR		RR		RR	RR	R	A	R	RR				F	C	F				RR	RR							F	F		RR										RR	F		R	C			RR	A
17H-3, 54–55	306.19		V	M	R	RR	RR	F		RR	RR		A	R					R	C	F					R							F	R		RR	RR	R			RR					RR	F	R	R	C			RR	A
17H-3, 57–58	306.22		V	M				R	RR	R	RR	RR	A	R	RR				R	F	F					RR	RR						C	F					RR				RR	RR		RR	C	RR	RR	F	R		RR	C
17H-3, 60–61	306.25		C	M	RR	R		F		R	RR		A		RR				RR	F	F						RR						F	C		RR					RR		RR			F	C	R	RR	F			R	C
17H-3, 63–64	306.28		V	M	R			R		RR	RR		A	F					R	C	F						RR						F	F		RR		R					RR	RR		RR	C	R	RR	C		RR	RR	C
17H-3, 66–67	306.31		V	M	RR	RR		R	RR	R	RR		A	RR					R	F	C				RR	RR	RR				RR		C	C		RR					RR					F	C	R	F	C	RR		R	F
17H-3, 68–69	306.33		C	M				RR		RR	RR		A	RR					R	C	F									RR	RR		C	C		R		RR			RR		RR	RR		RR	C	RR	R	F	RR		RR	F
17H-3, 70–71	306.35		A	M				R		RR	RR		A		RR				R	C	C								RR				C	C		RR					RR			RR		F	C	R	R	F	RR		RR	R
17H-3, 72–73	306.37		C	M	R	RR		R		RR	RR		A					RR	R	R	R						RR						C	C		F	RR			RR	RR	cf	RR			RR	C	RR	F	F	RR			F
17H-3, 74–75	306.39		V	M	RR	RR		RR		RR	RR		A	RR					R	F	R						RR				RR		C	C		R	RR		RR		R			RR			C	R	F	F			RR	R
17H-3, 75–76	306.40		V	M		RR		RR		RR	RR	RR	A	RR					R	C	R												C	C		R	RR				R					F	C	R	F	F			RR	R
17H-3, 78–79	306.43		C	M						RR	RR		A					RR	R	C	F									RR			C	C		RR					R		RR	RR			C	RR	R	F				F
17H-3, 80–81	306.45		C	M		RR			RR	RR	RR	RR	C						R	C	F	RR	RR										A	C		RR					R					RR	F	RR	RR	F			RR	R
17H-3, 83–84	306.48		V	M	R						RR	RR	A		RR	RR			R	R	R		RR								R		A	A		RR					R	RR	RR				F		R	F	RR			R
17H-3, 84–85	306.49		V	M	RR	R		RR	RR	R	RR		A					RR	R	F	R		RR								R		A	C		R	RR				R					F	F	R	F	F	RR			RR
17H-3, 85–86	306.50		C	M	RR	RR		RR	RR		RR		A	RR		RR	RR			C	R	RR					RR				RR		A	C		RR					RR						F	RR	F	F	RR			
17H-3, 86–87	306.51		C	M							RR	RR	C	R	RR	RR	RR			C	R		cf	RR					RR	RR	R		A	C		R				RR	R		RR	RR			C	RR	R	F				
17H-3, 87–88	306.52		V	M	R				RR		RR		C	F		RR			R	C	F	RR	cf	RR	RR						RR		A	C		F	RR				RR					RR	C	RR	R	F				RR
17H-3, 88–89	306.53		V	M							RR		C	F	RR	RR				F	R	RR						RR		RR			C	C		RR					RR	RR	RR			RR	C	RR	F	F				
17H-3, 89–90	306.54		C	M					RR	RR	RR	RR	C	F		RR		RR	RR	F	F	RR											C	C		R					R	RR					C	RR	F	F				RR
17H-3, 90–91	306.55		V	M		RR					RR		A	F	RR			RR	RR	C	F	RR	cf				RR						A	C		F					RR						C	R	F	F	RR			RR
17H-3, 91–92	306.56		V	M		RR				R	R	RR	A	R	RR	RR		RR		C	F	RR	RR	R			R						A	F		R					RR	RR				RR	C	RR	F	F	R		R	R

Table T1 (continued).

Core, section, interval (cm)	Depth (mcd)	Nannofossil zone	Total abundance	Preservation	*Biantholithus* spp.	*Biscutum* spp.	*Braarudosphaera* spp.	*Campylosphaera* spp.	*Chiasmolithus bidens*	*Chiasmolithus consuetus*	*Chiasmolithus solitus*	*Chiasmolithus* spp.	*Coccolithus pelagicus*	*Coccolithus* spp.	*Cruciplacolithus* spp.	*Discoaster anartios*	*Discoaster araneus*	*Discoaster lenticularis*	*Discoaster mohleri*	*Discoaster multiradiatus*	*Discoaster nobilis*	*Discoaster diastypus*	*Discoaster* cf. *D. lodoensis*	*Discoaster salisburgensis*	*Ellipsolithus distichus*	*Ellipsolithus macellus*	*Ericsonia* spp.	*Fasciculithus alanii*	*Fasciculithus clinatus*	*Fasciculithus hayi*	*Fasciculithus involutus*	*Fasciculithus thomasii*	*Fasciculithus tympaniformis*	*Fasciculithus* spp.	*Hornibrookina* spp.	*Markalius* spp.	*Neochiastozygus* spp.	*Neococcolithes* spp.	*Pontosphaera* spp.	*Prinsius* spp.	*Rhomboaster bramlettei* s.a.	*Rhomboaster bramlettei* l.a.	*Rhomboaster bramlettei* var. T	*Rhomboaster* cf. *R. contortus*	*Sphenolithus anarrhopus*	*Sphenolithus moriformis*	*Sphenolithus primus*	*Thoracosphaera* spp.	*Toweius eminens*	*Toweius pertusus*	*Toweius* spp.	*Tribrachiatus* cf. *T. digitalis*	*Placozygus* spp.	*Zygrhablithus bijugatus*
17H-3, 92–93	306.57	NP 10	C	M				RR			RR	R	A	F	RR	RR		RR	R	F	F	RR					RR	RR			R		A	C		R					RR					RR	F	RR	R	R	RR		R	
17H-3, 93–94	306.58		V	M						RR	RR	RR	A	F		RR			RR	C	R	RR		RR			R		RR	RR	RR	RR	A	C		R										F	F	RR	F	F	RR			
17H-3, 94–95	306.59		C	M		RR				R	RR		A	RR	RR	RR		RR	R	C	RR	RR	cf	RR			RR		R				A	F		RR					RR	RR				F	C	R	F	F				RR
17H-3, 95–96	306.60		C	M						R	RR	RR	A	R	R	RR	RR	RR		C	RR	RR		RR				RR			RR	RR	C	F		RR				R	RR					F	C	RR	F	R	R			RR
17H-3, 96–97	306.61		V	M						RR	RR	RR	A	RR	RR	RR			RR	C	F	RR	RR				R		RR			RR	A	F		RR					RR					F	C	RR	F	F	RR			
17H-3, 98–99	306.63		R	M							RR		A	RR		RR			RR	A	F		cf		RR		R	R	RR	R	R	RR	C	F												F	C	RR	R	R	F			RR
17H-3, 100–101	306.65		R	M						RR	R		A	R		RR		RR		C	R	cf	cf				F	R	R	RR	RR	RR	C	F		RR										RR	C	RR	F	F	F			
17H-3, 101–102	306.66		R	M						RR	RR		C			RR			RR	A	F												C	F							RR						F	RR	RR	F				
17H-3, 102–103	306.67		R	P							RR		F			RR	RR		RR	A	C												C	F													R		R	RR				
17H-3, 103–104	306.68		RR	P																C													C	C													C							
17H-3, 104–105	306.69		R	P							R		F							C	F												A	C							F						F			RR				
17H-3, 105–106	306.70		RR	P																RR																																		
17H-3, 106–107	306.71		R	P				RR			RR		C							C	F							RR				RR	A	F							RR								R	R				
17H-3, 107–108	306.72		R	P	R				RR	RR	RR		A			RR				C	F	cf					F	RR	R		R	RR	C	F		RR					RR					F	F	RR	F	F	R			
17H-3, 108–109	306.73		R	P							R		C	R						C	R						R						A	C												F	C	RR	R	F				
17H-3, 109–110	306.74	NP 9	R	P							RR	RR	A	RR		R	RR			C	R	cf					R	RR	R			RR	C	C		RR			R							F	C		F	F	RR			RR
17H-3, 110–111	306.75		RR	P							R		F			RR				F	R							R					A	R													C	RR	R	R				
17H-3, 111–112	306.76		RR	P																RR																													RR					
17H-3, 112–113	306.77		C	P	R			R	RR	R	RR	R	A						R	C	C				R						R		C	C					RR	RR						F	F		R	C			RR	
17H-3, 113–114	306.78		V	M	RR	RR		RR		R	R	R	A	RR	RR				R	C	F				RR		RR	RR	RR	RR	R		C	R		R	RR		R	R						F	C	R	C	C	R			RR
17H-3, 114–115	306.79		V	M		RR			RR	R	R	R	A		RR				R	C	C							RR		RR	RR		C	C					RR							RR	F		C	C				RR
17H-3, 115–116	306.80		V	M				RR	RR	R	RR	R	A		RR				RR	C	C								RR	RR			C	R			RR		RR	R						F	C		F	C	R		RR	
17H-3, 117–118	306.82		V	M	RR	R	RR		F	R	RR	R	A		RR				RR	C	F				RR			RR	RR	RR	RR		F	F			RR		R	R						RR	F	RR	F	C	RR		RR	R
17H-3, 119–120	306.84		V	M	RR	RR		RR	RR	R	R	R	A	R					R	C	R				R		RR		R		R		F	F			RR		R	F						F	C	R	F	C			R	RR
17H-3, 121–122	306.86		V	M		RR		RR	F	R	RR	RR	A	RR	RR				R	C	R				R				RR	RR	RR		F	F			RR		R	R						F	F	R	F	C	R		RR	F
17H-3, 123–124	306.88		V	M		RR		RR	RR	R	R	RR	A	RR	RR				R	C	F				R		RR			RR			F	F			RR		R	R						F	F	RR	F	A	RR		RR	F
17H-3, 127–128	306.92		V	M	RR	R	RR	RR	RR	R	F	R	A	RR					RR	C	F				R				RR				F	F					RR	R					RR	F	F	RR	C	C	R		RR	F
17H-3, 129–130	306.94		V	M		RR		R	RR	R	R	RR	A	R	R			RR	RR	F	F				RR	RR		RR	RR	RR	RR		F	F			RR	R	RR	F					RR	F	F	RR	F	C	R		R	R
17H-3, 131–132	306.96		V	M		RR		RR		RR	R	R	A		R				RR	C	F				RR		RR	RR					F	F			RR	R	R	R						F	C	RR	C	C	R		F	F
17H-3, 133–134	306.98		V	M		R	RR		RR	R	R	R	A		R				R	C	F				RR	RR			RR				C	R			RR		RR	RR						F	F	R	F	A	RR		RR	C
17H-3, 135–136	307.00		V	M		R		RR	RR	F	RR	RR	A		RR			RR	R	C	F				RR	RR	RR	RR	RR	RR			F	F			RR	RR	R	R						F	F	R	F	C	RR		F	F
17H-3, 137–138	307.02		V	M		R				RR	R	R	A						RR	C	F				RR				RR				F	F					R	F						F	F	RR	F	C	R		R	F
17H-3, 139–140	307.04		V	M		RR				RR	RR	RR	A		RR				R	F	R				RR	RR	RR	RR	RR	RR	RR		C	F			RR	RR	RR	F					RR	F	C	RR	C	C	RR		RR	R
17H-3, 141–142	307.06		V	M	R	RR				R	R		A		R				R	C	F				RR			R	RR		RR		C	F			RR		R	R						F	F	RR	F	C	R		R	F
17H-3, 143–144	307.08		V	M		RR		RR		R	RR		A		RR				R	C	R				RR		RR	RR	RR	RR			F	F			RR		RR	F						F	F		C	C	R		RR	F
17H-3, 145–146	307.10		V	M	R	RR				RR	R	RR	A		RR				RR	C	F				RR	RR	RR		RR		R		C	F			RR		R	R						F	F	RR	F	C			R	R
17H-3, 147–148	307.12		V	M	R	R		R		R	R		A		R			R	F	C	R				RR		R	RR	R		RR		C	R			R		R	F						F	F	RR	R	C			R	F
17H-3, 149–150	307.14		V	M	RR	R		RR		RR	R		A		R				F	C	R				RR	F	RR	RR		R	R		F	F			RR	F	R	F					R	F	F	R	C	C	RR		R	F

Notes: Nannofossil zones from Martini (1971). Abundance: V = very abundant, A = abundant, C = common, F = few, R = rare, RR = very rare, cf = compare. Shaded area = dissolution interval.

CHAPTER NOTE*

N1. Angori, E., Bernaola, G., and Monechi, S., in press. Calcareous nannofossil assemblages and their response to the Paleocene/Eocene Thermal Maximum Event at different latitudes: ODP Site 690 and Tethyan sections. *In* Monechi, S., Coccioni, R., and Rampino, M. (Eds.), *Large Ecosystem Perturbations: Causes and Consequences*. Spec. Pap.—Geol. Soc. Am.

---

*Dates reflect file corrections or revisions.